

This is the accepted manuscript made available via CHORUS. The article has been published as:

First On-Sky Fringes with an Up-Conversion Interferometer Tested on a Telescope Array

P. Darré, R. Baudoin, J.-T. Gomes, N. J. Scott, L. Delage, L. Grossard, J. Sturmann, C.
Farrington, F. Reynaud, and T. A. Ten Brummelaar

Phys. Rev. Lett. **117**, 233902 — Published 29 November 2016

DOI: [10.1103/PhysRevLett.117.233902](https://doi.org/10.1103/PhysRevLett.117.233902)

First fringes on the sky with an upconversion interferometer tested on a telescope Array

P. Darré,^{*} L. Delage, L. Grossard, and F. Reynaud[†]
*Xlim, Photonics Department, UMR CNRS 7252,
123 av. Albert Thomas, 87060 Limoges, France*

R. Baudoin
*Xlim, Photonics Department, UMR CNRS 7252,
123 av. Albert Thomas, 87060 Limoges, France and
Current address: Laboratoire Charles Fabry, UMR 8501,
Institut d'Optique, CNRS, University Paris Sud,
2 Avenue A. Fresnel, 91127 Palaiseau Cedex, France*

J.-T. Gomes
*Xlim, Photonics Department, UMR CNRS 7252,
123 av. Albert Thomas, 87060 Limoges, France and
Current address: Novae, Z.I. de Bel Air, 87700 Saint-Martin-le-Vieux, France*

N.J. Scott, J. Sturmann, C. Farrington, and T. Ten Brummelaar
The CHARA Array, Mt. Wilson Observatory, Mt. Wilson, CA 91023, USA
(Dated: September 30, 2016)

The Astronomical Light Optical Hybrid Analysis (ALOHA) project investigates the combined use of a telescope array interferometer and nonlinear optics to propose a new generation of instruments dedicated to high resolution imaging for infrared astronomy. The nonlinear process of optical frequency conversion transfers the astronomical light to a shorter wavelength domain. Here, we report on the first fringes obtained on the sky with the prototype operated at 1.55 μm in the astronomical H band and implemented on the Center for High Angular Resolution Astronomy (CHARA) telescope array. This seminal result allows us to foresee a future extension to the challenging mid-infrared spectral domain.

PACS numbers: 42.65.Ky, 42.50.Ex, 07.60.Ly, 42.65.Wi, 95.55.Cs

Many astronomical studies in the optical domain, such as Active Galactic Nuclei, Young Stellar Objects, formation and evolution of planetary systems require very accurate information in the order of milli-arcseconds. To achieve this level of performance, astronomical instruments have evolved from monolithic structures, with a maximum aperture diameter smaller than 10 m, to telescope arrays with a set of apertures separated by several hundred meters. In this operating framework, the observation of an astrophysical target does not produce classical images, but involves the analysis of the similarity between the optical waves collected by each elementary telescope through intensity [1, 2] or field correlation [3]. Currently, the most active instruments based on the field correlation are the Very Large Telescope Interferometer (VLTI) [4] and the Center for High Angular Resolution Astronomy (CHARA) Array [5].

Here we present a new kind of instrument called Astronomical Light Optical Hybrid Analysis (ALOHA). The astronomical light collected by each telescope is shifted in wavelength from the near-infrared to the visible domain. This frequency shift is applied in each interferometric arm thanks to a nonlinear optical stage, before the interferometric mixing and detection.

A signal wave coming from the astronomical target interacts in a nonlinear crystal waveguide with the pump laser. This interaction generates a converted optical field by sum frequency generation (SFG) [6]. The phase of the signal is copied to the converted one during the nonlinear process. This SFG process is well-known to be intrinsically noiseless as one signal photon and one pump photon must be involved to create an upconverted photon [7]. The pump laser has to be shared between the different interferometric arms to preserve the mutual coherence between the optical fields to be correlated through the interferometric mixing. In addition, SFG is highly spectrally selective when using a monochromatic pump laser, leading to a high spectral resolution. This increases the coherence length of the interferometric signal and gives access to important scientific applications in the domain of stellar physics where the combining of spectral capabilities with interferometric measurements are of primary importance [8, 9]. In a previous work [10], we demonstrated in laboratory that upconversion interferometry preserves spatial coherence analysis of a black-body source mimicking an astrophysical source in the photon counting regime. This paper reports on the first fringes obtained on the sky with ALOHA implemented on

the CHARA Array. The light of stars emitted at $1.55\ \mu\text{m}$ in the H band has been converted to the visible domain at $631\ \text{nm}$ in each arm of the interferometer before being mixed and detected in the photon counting regime.

EXPERIMENTAL SETUP

This proof-of-principle version of our instrument has been developed at $1.55\ \mu\text{m}$ operating wavelength (within the astronomical H band) to take advantage of efficient devices provided by the telecommunication domain [11, 12]. In the first step, the star light is collected by two 1-m diameter telescopes of the CHARA Array (Fig. 1). Tip-tilt stages, located just after the telescope foci, stabilise the beams to efficiently couple the incident waves in the instrument. The free-space propagation of the optical fields reach the CHARA Array delay lines. The ALOHA instrument is implemented in a room next to the CHARA Array focal laboratory. Two 14-m long silica fibres link the two rooms and constitute the two interferometric arms of the infrared stage. They are plugged to the CHARA Array thanks to the Fiber Linked Unit for Optical Recombination (FLUOR) injection modules [13] in the focal laboratory. Raster scans allow us to set the fibre tip at a position where the coupled intensity is maximised by using either an internal reference source during the preparation of an observing run or the astronomical target itself when observing. Throughout the instrument, the propagation and the spatial mode filtering are ensured by using polarisation maintaining single-mode waveguides. The infrared stellar light is then guided through the infrared stage. The latter includes a fibre optical path modulator to scan the interferometric signal as a function of time by applying a linear variation of the optical path on a piezoelectric module. In the second step, the frequency conversion takes place in periodically poled lithium niobate (PPLN) waveguides provided by NTT Corporation, implemented on each arm of the interferometer. The waveguides are 22-mm long and pigtailed with fibres at the input and the output of the device, improving the reliability and the efficiency of the light coupling. They convert a 0.6-nm bandwidth of the astronomical signal centred at $1.55\ \mu\text{m}$ to the visible domain at $631\ \text{nm}$. The process is powered by a monochromatic pump source at $1.064\ \mu\text{m}$ equally shared between the two arms of the interferometer thanks to a 50/50 fibre coupler.

In the third step, the two outcoming beams are combined through a 2×2 fibre optic coupler providing two π phase-shifted interferometric signals. To fit the faint astronomical source detection requirements, the detection is performed using two Si-APD photon counters (70% quantum efficiency and 50Hz darkcount rate). The outcoming interferometric signals need to be spectrally filtered since parasitic processes, such as frequency dou-

bling of the pump at $532\ \text{nm}$ and residual signal of pump, may disturb the science signals. Notice that, even after a spectral selection around the converted signal wavelength domain, a cascade of spontaneous parametric down-conversion of the pump and SFG process induces a quadratic parasitic signal as a function of the pump power level [14].

Although the overall internal quantum efficiency of the PPLNs can reach 90% for a polarized source, as reported in [15], the best signal-to-noise ratio (SNR) is obtained with a trade-off between the SFG conversion efficiency and this extra background level. In our experimental configuration, the global power conversion efficiency of each conversion stage is typically equal to $\eta = 6\%$ for a linearly polarized source with a 1.2 kHz noise count rate and a pump power equal to 30mW. This value takes the PPLN nonlinear conversion efficiency into account, but also the coupling efficiency between the fiber and the nonlinear waveguide at the input and output of the component.

DATA PROCESSING AND RESULTS

The two telescopes S1–S2 of the CHARA Array, defining a baseline of 34 m, were used to achieve the observing run during two nights. A procedure was set up to make an observation sequence composed of the following raw data acquisitions:

- "beams 1+2": the interferometric signal acquisition. At the end of a measurement, we obtain two data files related to the two π -phased shifted interferometric outputs;
- "beam 1" or "beam 2": the photometric level acquisition of a single beam. The star light is injected only in one arm of the interferometer;
- "off-source": the dark count level acquisition without star light injection into the two ALOHA's inputs. The nonlinear crystals are fed by the pump laser source. This additional background signal is due to the spontaneous parametric down-conversion generated by the pump during the nonlinear process and the dark count of the Si-APD detector.

The "off-source" acquisition is performed at the beginning and at the end of each run to evaluate the stability of the flux delivered by the pump source.

Data processing

The raw data consist of two sets of N frames (one per interferometric output) of binary functions $X_i^d(t)$, $i \in$

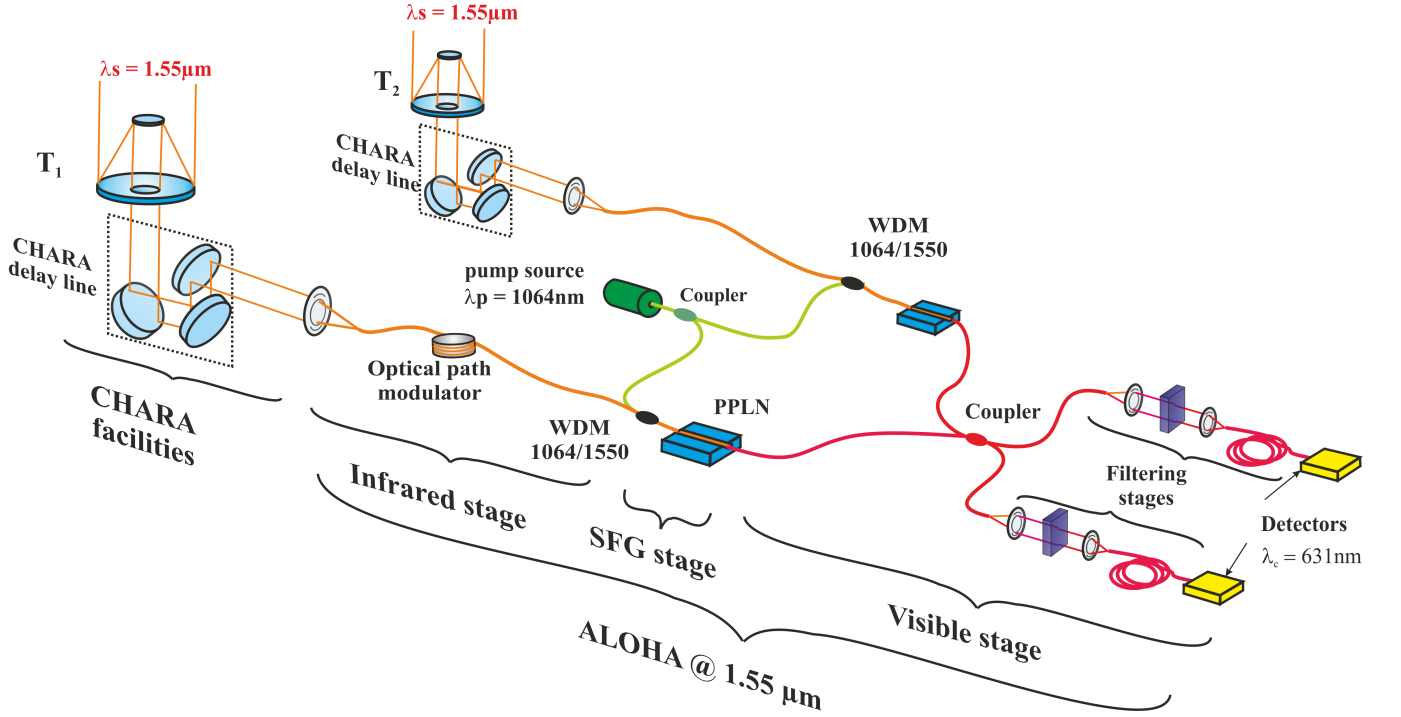


FIG. 1. On-site configuration with implementation of the ALOHA prototype at 1.55 μm on the CHARA Array. It is composed of three different stages (infrared, SFG and visible stages). Apart the filtering stage, the interferometer is entirely fibred with single-mode and polarisation maintaining fibres.

$[1, N]$, where d denotes the interferometric output index (1 or 2). Each frame is recorded over an acquisition time $\tau = 0.2$ s, and processed by a fast Fourier transform to get

$$\tilde{X}_i^d(f) = \text{FFT}[X_i^d(t)]. \quad (1)$$

where $\tilde{X}_i^d(f)$ is the spectrum associated to a temporal frame.

In this interferometric mode, the piston error due to the atmospheric turbulence induces a random fluctuation of the fringe pattern position. It is therefore necessary to integrate on the squared modulus of the spectrum (incoherent integration) also denoted power spectral density (PSD). Notice that the fringe modulation frequency is experimentally set to 110 Hz to keep the fringe peak on the PSD out of range of intensity fluctuations due to atmospheric turbulence or any other disturbance sources like vibrations generated by the air conditioning. Thanks to the spectral bandwidth of the SFG process (0.6 nm), the related coherence length of the converted field is then equal to 4 mm corresponding to approximately 2600 fringes in the fringe envelope. The temporal modulation amplitude of the optical path difference allows us to record 22 fringes per frame, which represents less than 1% of the fringe envelope. This ensures that the fringe visibility remains constant over each acquisition frame.

Furthermore the two interferometric outputs of the recombination coupler are intrinsically in phase opposition. Thus, by subtracting the two outputs frame simultaneously acquired, the power spectrum gives the integrated peak at the fringe modulation frequency f_{mod} . The corresponding data processing is adapted using the following equation

$$\langle |\tilde{X}(f)|^2 \rangle = \frac{1}{N} \sum_{i=1}^N |\tilde{X}_i^1(f) - \tilde{X}_i^2(f)|^2 \quad (2)$$

where N is the number of frames.

Because of the low stellar flux, it was necessary to integrate the PSD over a long time to reduce the influence of statistical noise and thus increase the SNR of the measurement, which can be written as

$$\text{SNR} = \frac{\langle |\tilde{X}(f_{\text{mod}})|^2 \rangle - \langle N_c \rangle}{\text{RMS}(\langle |\tilde{X}(f)|^2 \rangle)} \quad (3)$$

Equation 3 represents the ratio between the modulated peak amplitude at f_{mod} corrected from the background $\langle N_c \rangle$ corresponding to the mean number of electrical pulses detected per frame. The fluctuation of this white noise background, denoted $\text{RMS}(\langle |\tilde{X}(f)|^2 \rangle)$, is evaluated in a frequency slot at far away from the fringe modulation frequency f_{mod} .

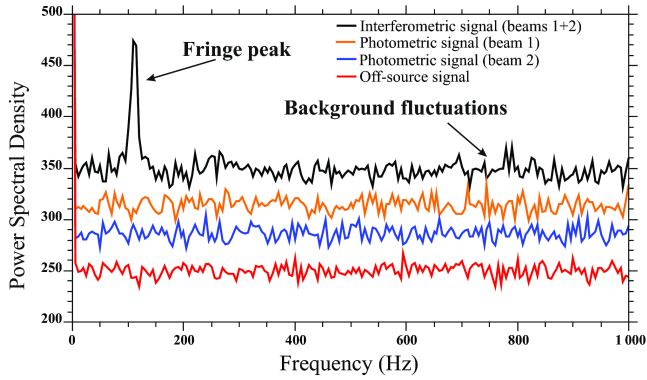


FIG. 2. Experimental power spectral density (PSD) related to the α UMa interferogram. Black : interferometric configuration, blue and orange : photometric signals, red : interferometric configuration without signal source.

First fringes on the sky

On the night of April 19th 2015, our prototype detected fringes on α Ursae Majoris (HD 95689) of -0.6 magnitude in H band, as presented on Fig. 2. The four curves represent the integration of the power spectrum related to each configuration of the observation sequence. The measurements were achieved over a 2000 frame integration with 0.2 s duration per frame. The fringe modulation frequency was set to 110 Hz.

A peak standing out from the noise background is only observed on the interferometric signal acquisition (black curve). This is the evidence of interferences modulated at 110 Hz and can not result from any spurious modulation. This clearly demonstrates the first observation of interferometric fringes with the ALOHA instrument implemented on the CHARA Array.

The modulation peak is spread around 110 Hz over several frequency channels because of the optical path variations due to the atmospheric turbulence during the measurements. The differential longitudinal phase fluctuations between the two telescope apertures, not filtered out by single-mode optical fibres, leads to a phase modulation of the fringes as a function of time. Hence, the fringe peak is integrated to collect all the information related to the astronomical object.

The SNR evolution of the fringe peak amplitude as a function of time is shown in Fig. 3. The uneven SNR evolution is due to the atmospheric turbulence leading to fluctuation of the coupling efficiency into the fibres. Integrating the full fringe peak, the SNR is equal to 62 over a 400 s integration time. The SNR curve follows the theoretical root mean square evolution as a function of the integration time, whereas the other curves remain close to zero. This corroborates the detection of the interferometric signal.

Table I shows the experimental results obtained for

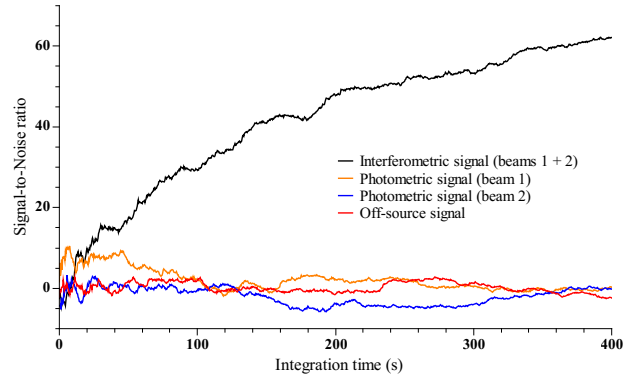


FIG. 3. Comparison of the signal-to-noise ratio measured in interferometric and in photometric configurations. In the photometric configurations, the flux level is measured by injecting the light in one single-arm, one after the other, and then without light injection at the input of the interferometer.

TABLE I. Summary of the observations results. The mean value of atmospheric coherence length r_0 estimated at 550 nm is about 11 cm during the nights of April 19th and 20th 2015.

Object	Hmag	date	ΔT (sec)	SNR
HD 95689	-0.6	2015 April 19	400	62
HD 121370	1.4	2015 April 19	1500	15
HD 128333	2.0	2015 April 19	1500	9
HD 163113	3.0	2015 April 20	1500	7

four stars observed during the nights of April 19th and 20th 2015. The atmospheric coherence length r_0 at 550 nm is estimated at 11 cm, corresponding to a moderate seeing of approximately $1.0''$ for the two nights. SNR values are obtained by integrating the fringe modulation peak over 55 Hz around 110 Hz.

We reached a limiting magnitude (i.e. the faintest observable source) of 3 with an integration time of 1500s and a spectral bandwidth equal to 0.6 nm, that would correspond to a spectral resolution of 2600. By way of comparison, MIRC (Michigan InfraRed Combiner) is a mature fiber-based combiner operating at the CHARA Array since 2005, and routinely gives astrophysical results in the H band. References [16, 17] report a limiting magnitude equal to 4.5 in H band when observing with a 42 spectral resolution and over a 120 to 300 s integration time. These current experimental results obtained with ALOHA are promising. In comparison with MIRC, the power sensitivity is only smaller by a factor of four (magnitude difference equal to 1.5), but with a greater spectral resolution by a factor 60.

CONCLUSION AND PERSPECTIVES

We have reported on the first fringes obtained during observations on the sky with a high resolution imaging instrument including a nonlinear frequency conversion in

each interferometric arm. The first result was achieved around $1.55\ \mu\text{m}$ with a stellar source of magnitude -0.6 with a SNR of 62 over a 400 s integration time. The bandwidth of the infrared field converted by SFG was about 0.6 nm, that would lead to a spectral resolution equal to 2600. We detected fainter sources up to magnitude $+3$ (HD 163113) with a SNR of about 7 by integrating the full modulation peak over about 25 min. Although this study is an on-the-sky proof of principle of the ALOHA concept in H band, we have been able to detect fringes on real stars with performances comparable to state-of-the-art methods.

The long term development will be focused to longer wavelengths ranging from 3 to $12\ \mu\text{m}$, corresponding to the astronomical L, M and N bands. We obtained first promising in-lab results at $3.39\ \mu\text{m}$ [18]. In this context, the ALOHA concept is of particular interest and offers several advantages. Implementing the upconversion process as close as possible to the telescope focus would allow us to substantially reduce the contribution of the thermal emission of all the optical components downstream the nonlinear process as shown in figure 4. In this case, the delay lines and optical path modulator can be used after the nonlinear stage as the phase of the signal photons is preserved during the SFG process as shown in [19]. Once shifted to the visible or near-infrared spectral domain, the converted beams coming from the conversion stages can be efficiently processed using silica optical fibres or guided optics. This offers an efficient solution for spatial filtering [4, 20] and coherent light transport over a long-distance (including fibred delay line), and enables the use of compact and reliable combiners. As the SFG process is achieved over a narrow spectral bandwidth, such an instrument will benefit from a high spectral resolution, which is not available with a classical instrument without a strong reduction of its sensitivity. Finally, the upconversion process allows the use of relatively low-cost and high-performance photon counting detectors with high quantum efficiency, and low dark count, compared to their more expensive and complex equivalents in the mid-infrared domain.

ACKNOWLEDGMENTS

This work is supported by the Centre National d'Études spatiales (CNES), Thales Alenia Space and the Institut National des Sciences de l'Univers (INSU). Operational funding for the CHARA Array is provided by the Georgia State University College of Arts and Sciences and by the National Science Foundation through Grant AST-1211129. We would like to acknowledge Alain Dextre for his advice and the realisation of the mechanical parts. Our thanks go to Denis Mourard and Pierre Léna for fruitful discussions and encouragements.

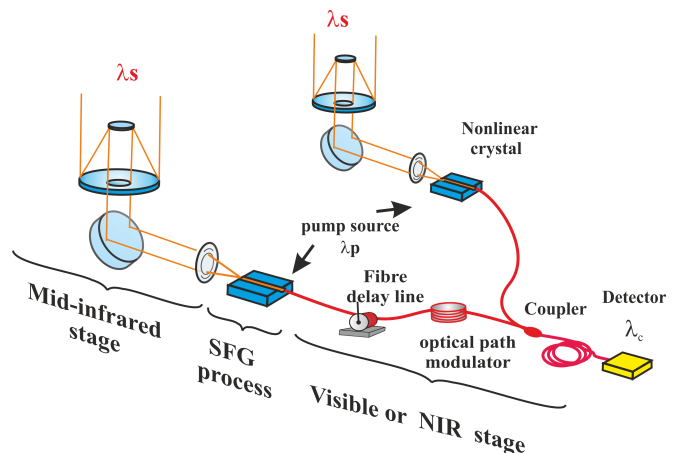


FIG. 4. Future design for the mid-infrared domain. The light collected by the telescopes are upconverted in nonlinear crystals as close as possible to the telescope foci, before being mixed thanks to a fibred coupler.

* pascaline.darre@etu.unilim.fr

† francois.reynaud@unilim.fr

- [1] R. H. Brown and R. Q. Twiss, *Nature* **178**, 1046 (1956).
- [2] M. A. Johnson, A. L. Betz, and C. H. Townes, *Physical Review Letters* **33**, 1617 (1974).
- [3] J. D. Monnier, *Reports on Progress in Physics* **66**, 789 (2003).
- [4] R. G. Petrov, F. Malbet, G. Weigelt, P. Antonelli, U. Beckmann, Y. Bresson, A. Chelli, M. Dugu, G. Duvert, and G. et al., *Astronomy and Astrophysics* **464**, 1 (2007).
- [5] T. A. t. Brummelaar, H. A. McAlister, S. T. Ridgway, J. W. G. Bagnuolo, N. H. Turner, L. Sturmann, J. Sturmann, D. H. Berger, C. E. Ogden, R. Cadman, W. I. Hartkopf, C. H. Hopper, and M. A. Shure, *The Astrophysical Journal* **628**, 453 (2005).
- [6] R. W. Boyd, *Optical Engineering* **16**, 166563 (1977).
- [7] W. H. Louisell, A. Yariv, and A. E. Siegman, *Physical Review* **124**, 1646 (1961).
- [8] B. Lopez, S. Lagarde, P. Antonelli, W. Jaffe, R. Petrov, L. Venema, S. Robbe-Dubois, F. Bettonvil, P. Berio, and R. e. a. Navarro, in *SPIE Astronomical Telescopes+ Instrumentation* (International Society for Optics and Photonics, 2012) pp. 84450R–84450R.
- [9] D. Mourard, P. Brio, K. Perraut, R. Ligi, A. Blazit, J. M. Clausse, N. Nardetto, A. Spang, I. Tallon-Bosc, and B. et al., *Astronomy & Astrophysics* **531**, A110 (2011).
- [10] J.-T. Gomes, L. Delage, R. Baudoin, L. Grossard, L. Bouyeron, D. Ceus, F. Reynaud, H. Herrmann, and W. Sohler, *Physical Review Letters* **112**, 143904 (2014).
- [11] L. Del Rio, M. Ribiere, L. Delage, and F. Reynaud, *Optics Communications* **281**, 2722 (2008).
- [12] S. Brustlein, L. Del Rio, A. Tonello, L. Delage, F. Reynaud, H. Herrmann, and W. Sohler, *Physical Review Letters* **100**, 153903 (2008).
- [13] N. J. Scott, R. Millan-Gabet, E. Lhom, T. A. Ten Brummelaar, V. Coud Du Foresto, J. Sturmann, and L. Sturmann, *Journal of Astronomical Instrumentation* **02**,

- 1340005 (2013).
- [14] J. S. Pelc, C. Langrock, Q. Zhang, and M. M. Fejer, *Optics Letters* **35**, 2804 (2010).
 - [15] R. V. Roussev, C. Langrock, J. R. Kurz, and M. M. Fejer, *Optics Letters* **29**, 1518 (2004).
 - [16] E. Pedretti, J. D. Monnier, T. t. Brummelaar, and N. D. Thureau, *New Astronomy Reviews Proceedings: VLTI summerschool*, **53**, 353 (2009).
 - [17] N. D. Richardson, G. H. Schaefer, D. R. Gies, O. Chesneau, J. D. Monnier, F. Baron, X. Che, J. R. Parks, R. A. Matson, Y. Touhami, D. P. Clemens, E. J. Aldoretta, N. D. Morrison, T. A. ten Brummelaar, H. A. McAlister, S. Kraus, S. T. Ridgway, J. Sturmann, L. Sturmann, B. Taylor, N. H. Turner, C. D. Farrington, and P. J. Goldfinger, *The Astrophysical Journal* **769**, 118 (2013).
 - [18] L. Szemendera, P. Darré, R. Baudoin, L. Grossard, L. Delage, H. Herrmann, C. Silberhorn, and F. Reynaud, *Monthly Notices of the Royal Astronomical Society* **457**, 3115 (2016).
 - [19] J.-T. Gomes, L. Grossard, D. Ceus, S. Vergnole, L. Delage, F. Reynaud, H. Herrmann, and W. Sohler, *Optics express* **21**, 3073 (2013).
 - [20] J.-B. Le Bouquin, J.-P. Berger, B. Lazareff, G. Zins, P. Haguenauer, L. Jocou, P. Kern, R. Millan-Gabet, W. Traub, and O. e. a. Absil, *Astronomy and Astrophysics* **535**, A67 (2011).